Military Technical College,
Kobry El-Kobbah,
Cairo, Egypt

9th International Conference
On Aerospace Sciences &
Aviation Technology

GEOMETRIC ANALYSIS OF CRUCIFORM AND TRIFORM SOLID PROPELLANT GRAINS

ZAYED* A-N.

ABSTRACT

This paper describes criteria and formulas that are capable of evaluating the burning perimeters of cruciform and triform solid propellant grains (externally burning grains) during combustion. The effect of the restrictor width on the burning perimeter during combustion is investigated and analyzed. Some dimensions of the grain configuration are optimized and recommended.

KEY WORDS

Rocket motor, Solid propellant, Cruciform grain, Triform grain.

NOMENCLATURE

$A_{1,2,..}$	area of propellant sectors	y	burnt distance
A_c	combustion chamber cross sectional area	$\bar{y}$	dimensionless parameter = y/b
A_f	free area (port area)	α	web angle
A_p	propellant area	δ	restrictor thickness
A_s	sliver area	φ	leg angle in a triform grain
$a_{1,2,..}$	segments of burning perimeter		
b	web thickness		
K_{FC}	filling coefficient		
n	number of legs		
R_1	inner radius of rocket motor		
R_2	outer radius of grain		
S	burning perimeter		
S_o	initial burning perimeter		
S_s	sliver perimeter		
$\bar{S}$	dimensionless parameter = S/R_2		
x	restrictor width		

INTRODUCTION

The cruciform and triform grains are classified in grain configuration as externally burning grains where the burning is on the external surface of the grain. The burning perimeter is divided into different segments. Some of these segments are created during burning and others are vanished. Therefore, during combustion, the change in the burning perimeter results in different phases of combustion.

All dimensions of the grain configuration are related to R_2. Some of these dimensions have recommended values[1], these values are studied to know the effect of their variation on the burning performance and the ballistic coefficients of the rocket motor.

FLAT SURFACE GRAINS

This grain may be found in two configurations, the first is a three-leg (triform) grain and the second is a four-leg (cruciform) grain, as shown in Fig.1.

Main Dimensions

The most important dimension of this grain, as shown in Fig. 2, is the web thickness "b" which is related to R_2 as,

Three-leg: $b = 0.374\ R_2 \longrightarrow \alpha \approx 21.93^\circ$

Four-leg: $b = 0.314\ R_2 \longrightarrow \alpha \approx 18.28^\circ$

These values of the web thickness lead to optimum filling coefficient ($K_{FC} = 0.85$) as recommended in [1,2] for solid propellant rocket motors with single-grain. All other dimensions are related to R_2 or b, such as:

– the restrictor width "x" is taken equal b.
– the restrictor thickness δ is taken $\approx 0.025R_1$ which leads to $D_2 \approx 0.95D_1$.

The filling coefficient is calculated as

$$K_{FC} = \frac{A_p}{A_c} \tag{1}$$

where $A_c = \pi^2 R_1^2$, and the propellant area A_p is calculated as shown in Fig. 3 as,

$$A_p = 2n(A_1 + A_2 + A_3)$$

$$= 2n\left[\frac{R_2^2}{2}\left(\alpha - \frac{\sin 2\alpha}{2}\right) + b\left(R_2 \cdot \cos\alpha - b \cdot \cot\frac{\pi}{n}\right) + \frac{1}{2}b^2 \cdot \cot\frac{\pi}{n}\right] \tag{2}$$

Burning Perimeter

For x = b, three phases of burning can be distinguished during the course of regression of the web.

At start of burning

As illustrated in Fig. 4(a), the initial burning perimeter is

$$S_o = 2n(a_{20} + a_{30}) = 2n\left[R_2 \cdot \frac{\alpha}{2} + R_2 \cdot \cos\alpha - b \cdot \cot\frac{\pi}{n}\right] \quad (3)$$

During first phase

The conditions of the first phase is that $y \le \frac{b}{2}$ and $(\theta \ge \frac{\alpha}{2})$. As shown in Fig. 4(b), the burning perimeter is calculated as follows

$$S = 2n\,(a_1 + a_2 + a_3 + a_4) \quad (4)$$

where

$$a_1 = y\left(\frac{\pi}{2} - \frac{\alpha}{2} + \varepsilon\right) \quad (4.1)$$

$$a_2 = (R_2 - y)\left(\theta - \frac{\alpha}{2}\right) \quad (4.2)$$

$$a_3 = (R_2 - y) \cdot \cos\theta - b \cdot \cot\frac{\pi}{n} \quad (4.3)$$

$$a_4 = y\left(\frac{\pi}{2} - \frac{\pi}{n}\right) \quad (4.4)$$

$$\theta = \sin^{-1}\left(\frac{b - y}{R_2 - y}\right) \quad (4.5)$$

$$\varepsilon = \tan^{-1}\left(\frac{2\left(R_2 - \sqrt{R_2^2 - (b^2/4)}\right)}{b}\right) \quad (4.6)$$

During second phase

The conditions for the second phase is $\frac{1}{2} < \frac{y}{b} \le \frac{1}{2 - (b/R_2)}$ and $(\theta \ge \frac{\alpha}{2})$.

As presented in Fig. 4(c), the burning perimeter is computed as in the following form.

$$S = 2n\,(a_{12} + a_2 + a_3 + a_4) \quad (5)$$

Where

$$a_{12} = y \,.\, \psi = y\left(\frac{\pi}{2} - \frac{\alpha}{2} - \lambda\right) \quad (5.1)$$

$$\lambda = \tan^{-1}\left(\frac{\sqrt{4y^2 - b^2}}{b}\right) \tag{5.2}$$

and a_2, a_3, and a_4 are the same as in the first phase.

During third phase

The condition of the third phase is $y > b/2$ and $a_2 = 0$. As shown in Fig. 4(d), the burning perimeter is obtained as,

$$S = 2n\,(a_{13} + a_{33} + a_4) \tag{6}$$

Where $$a_{13} = y \,.\, \psi \tag{6.1}$$

ψ is the angle between AB and AC, as shown in Fig. 4(d). Let m_1 be the slope of AB and m_2 be the slope of AC.

$$\psi = \tan^{-1}\left(\frac{m_2 - m_1}{1 + m_1 \cdot m_2}\right) \tag{6.2}$$

where $m_2 = \tan\lambda$ as defined in Eq.(5.2), and

$$m_1 = \frac{\sqrt{4by - b^2}}{2y - b} \tag{6.3}$$

$$a_{33} = \sqrt{R_2^2 - \frac{b^2}{4}} - \sqrt{by - \frac{b^2}{4}} - b \cdot \cot\frac{\pi}{n} \tag{6.4}$$

The segment a_4 is the same as in the first and second phases.

The sliver

The sliver perimeter depends mainly on the grain diameter and the number of legs.

$$S_s = \pi b(n - 2) \tag{7}$$

The sliver area is calculated as,

$$A_s = nb^2\left(\cot\frac{\pi}{n} - \frac{\pi}{2} + \frac{\pi}{n}\right) \tag{8}$$

Table 1 shows the perimeter and area of sliver in a dimensionless form.

Table 1. Sliver perimeter and area of flat surface grains

	3-Leg	4-Leg
$\frac{S_s}{R_2}$	1.1735	1.973
$\frac{A_s}{R_2^2}$	0.0225	0.0846

The sliver area, of a 4-leg grain, is greater than that of a 3-leg grain by a factor of about 3.76 when the two grains have the same diameter.

This calculation procedure is implemented as a FORTRAN program to calculate the burning perimeter through the variation of the burnt distance y from 0 to b. Figure 5 presents the output of the program as a relation between two dimensionless parameters ($\bar{S}$ = S/R –vs– $\bar{y}$ = y/b). This curve shows that:

- the first phase is progressive, the second phase is sharply regressive, and the third phase is smoothly regressive.
- when comparing two grains (one 4-leg and another 3-leg) of the same diameter and the same filling coefficient, the burning perimeter of the 4-leg grain is always greater than that of the 3-leg grain. From the other hand, the web thickness (consequently, the burning time) of the 3-leg grain is greater than that of the 4-leg grain.

Variation of Restrictor Width

The restrictor width "x" is recommended in [1] to be equal to the web thickness "b". That is taken into consideration in the previous calculation of the burning perimeter. In this section, the program calculates the burning perimeter at two different values of restrictor width (x = 1.4b and x = 2b). Figure 6 shows the variation of the burning perimeter, for a 4-leg grain, at different values of the restrictor width. That figure demonstrates that the increase in the restrictor width increases the duration of the first phase. Also, the drop of the burning perimeter, after the first phase, is more sharp at greater restrictor width. In the case of full restrictor (x = 2b), the burning is described by one progressive phase.

CORRUGATED SURFACE GRAINS

This grain is found also in two configurations as a 3-leg (triform) and 4-leg (cruciform) grains, as shown in Fig. 7. The main dimensions of the grain are illustrated in Fig. 8, where all of these dimensions are related to the web thickness "b" which, in turn, is related to R_2. The leg angle $\varphi = \pi/2n$. To obtain the shown configurations, the web thickness is recommended to be taken as,

– for 3-leg grain	$b = 0.33333\ R_2$	$\longrightarrow$	$\alpha = 19.5^\circ$
– for 4-leg grain	$b = 0.27277\ R_2$	$\longrightarrow$	$\alpha = 16.0^\circ$

The restrictor width is recommended in [1] to be double the web thickness (x = 2b) and the restrictor thickness δ is taken $\approx 0.025R_1$. The mentioned values of the web thickness lead to filling coefficient as follows:

$K_{FC} = 0.607$ for 3-leg grains
$K_{FC} = 0.616$ for 4-leg grains

where the propellant areas (see Fig. 9) are calculated as,

$$A_p = 2n(A_1 + A_2 + A_3) \tag{9}$$

where $A_1 = \frac{1}{2}R_2^2\left(\frac{\pi}{2n}\right)$ $\qquad A_2 = \frac{1}{2}(R_2 - b)\frac{b}{\cos\left(\frac{\pi}{2} - \frac{\pi}{n}\right)} \cdot \sin\left(\frac{\pi}{2n}\right)$

$A_3 = \frac{1}{2}(b - \Delta)^2 \cdot \sin\left(\pi - \frac{\pi}{n}\right)$; $\qquad \Delta_{(n=3)} = b \cdot \frac{\sin\frac{\pi}{2n}}{1 + \sin\frac{\pi}{2n}}$; $\qquad \Delta_{(n=4)} = b \cdot \frac{\tan\frac{\pi}{2n}}{1 + \tan\frac{\pi}{2n}}$

The Burning Perimeter

For x = 2b, as the burnt distance increases, two burning phases can be distinguished.

At start of burning

As presented in Fig. 10(a), the initial burning perimeter is

$$S_o = 2n(a_{02} + a_{03} + a_{05} + a_{06}) \tag{10}$$

where $a_{02} = R_2(\varphi - \alpha)$ $\qquad a_{05} = a_{06} = b - \Delta$ (for n = 3)
$a_{03} = b$ $\qquad a_{05} = a_{06} = (b - \Delta)/\cos(\pi/2n)$ (for n = 4)

During first phase

As shown in Fig. 10(b), the conditions of the first phase are "$a_2 > 0$" and "$\beta > \alpha$". The burning perimeter is calculated as,

$$S = 2n(a_{11} + a_{12} + a_{13} + a_{14} + a_{15} + a_{16} + a_{17}) \tag{11}$$

where $a_{11} = y \cdot \left(\frac{\pi}{2} - \alpha + \varepsilon\right)$ $\qquad \varepsilon = \tan^{-1}\left(\frac{R_2 - \sqrt{R_2^2 - b^2}}{b}\right)$

$a_{12} = (R_2 - y)(\beta - \alpha)$ $\qquad a_{13} = b - y$

$a_{14} = a_{17} = y \,.\, \pi/n$ $\qquad a_{15} = a_{16} = b - \Delta - y \cdot \tan\frac{\pi}{2n}$

During second phase

The condition of the second phase is "$\beta < \alpha$". The burning perimeter, as shown in Fig.10(c), is calculated as follows:

$$S = 2n(a_{21} + a_{23} + a_{24} + a_{25} + a_{26} + a_{27}) \quad (12)$$

where $a_{21} = y \cdot (\lambda + \varepsilon)$ $a_{23} = \overline{BC}$ as shown in Fig.10(c)

$a_{24} = a_{27} = a_{14}$ as in first phase.

$a_{25} = a_{26} = a_{15}$ as in first phase.

The steps, of calculating the burning perimeter of a corrugated surface grain, are implemented as a FORTRAN program to calculate the burning perimeter as function of the burnt distance. Figure 11 shows the variation of $\bar{S}$ versus $\bar{y}$ for corrugated surface grains of 3 legs and 4 legs. That figure shows that:

- In the case of a 3-leg grain, the burning is generally quasi-neutral.
- In the case of a 4-leg grain, the first phase is slightly progressive while the second phase is highly progressive.
- The perimeter of a 4-leg grain is always greater than that of the 3-leg grain, while the web thickness of the 4-leg grain is less than that of the 3-leg grain.

The Sliver

To calculate the sliver perimeter, substitute in Eq. (12) by "y = b." The sliver area is calculated by subtracting the burnt propellant area from the initial propellant area. Table 2 presents in dimensionless form the sliver perimeter and area.

Table 2. Sliver perimeter and area of corrugated surface grains

	3-Leg	4-Leg
$\frac{S_s}{R_2}$	6.157	8.060
$\frac{A_s}{R_2^2}$	0.152	0.165

Variation of Restrictor Width

The description of corrugated surface grains[1] recommends that the restrictor width x = 2b. This section studies the burning perimeter at two different restrictor widthes (x = 1.3b and x = b). Such choices imply burning in three different phases, as illustrated in Fig.12, where:

-- the first phase is approximately neutral,

-- the second phase is regressive, and

-- the third phase is approximately neutral.

During the first phase, the decrease of restrictor width decreases the duration and gives geater burning perimeter. It also decreases the sliver perimeter and area of the grain.

In the case of full restrictor, where the restrictor covers the outer circumference of the grain, the burning becomes as a single progressive phase. That is represented by the dashed line in Fig. 12. Full restrictor leads to larger sliver area as compared to the other cases.

CONCLUSIONS

(1) The burning of flat surface grains has three phases; the first is pogressive, the second is highly regressive, and the third is smoothly regressive.

(2) The sliver perimeter and sliver area of a 3-leg flat surface grain are smaller than those of the 4-leg grain.

(3) The burning of corrugated surface grains has two phases; the first phase is approximately neutral and the second phase is progressive.

(4) The sliver perimeter and area, of a 3-leg corrugated surface grain, are smaller than those of the 4-leg grain.

(5) For flat surface grains, an increase in restrictor width decreases the burning perimeter and increases the duration of the progressive phase.

(6) For corrugated surface grains, any decrease in restrictor width increases the burning perimeter and decreases the duration of the first phase.

(7) In the case of full restrictor, both flat surface and corrugated surface grains burn as a single progressive phase.

REFERENCES

[1] Smolik, J and Ludvik, F., "Theory and Design of Rockets," MTC, Part II-a, Cairo, 1967.

[2] Smolik, J and Ludvik, F., "Theory and Design of Rockets," MTC, Part II-b, Cairo, 1967.

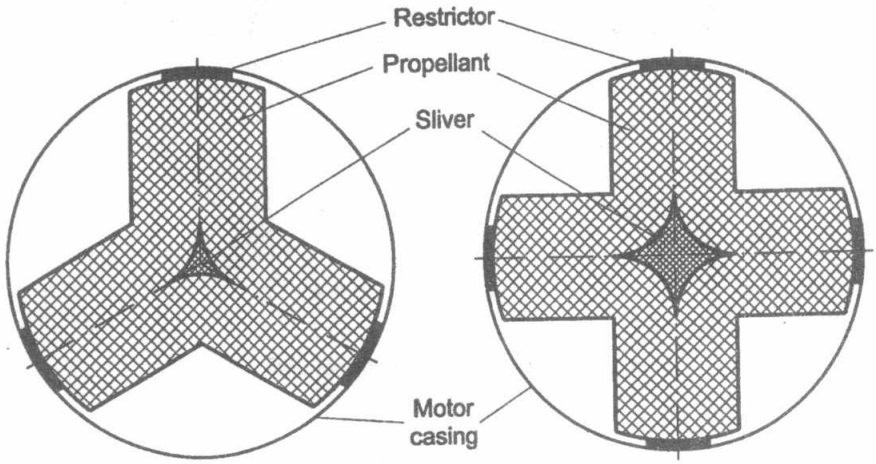

Fig. 1 Configuration of flat surface grains

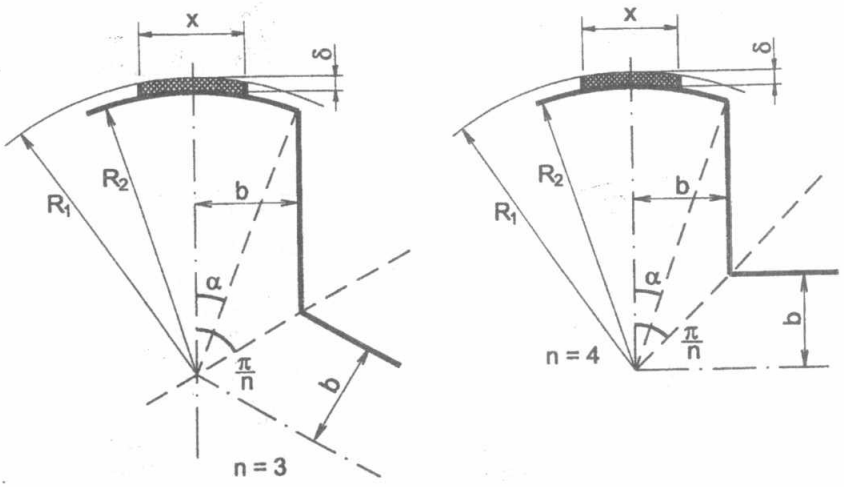

Fig. 2 Main dimensions of flat surface grains

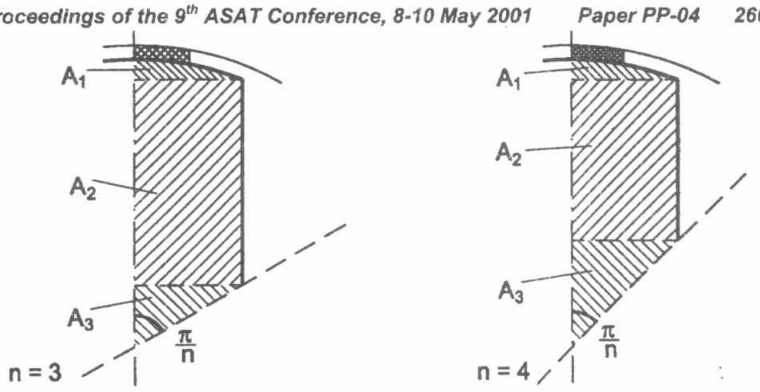

Fig. 3 Propellant cross-sectional area

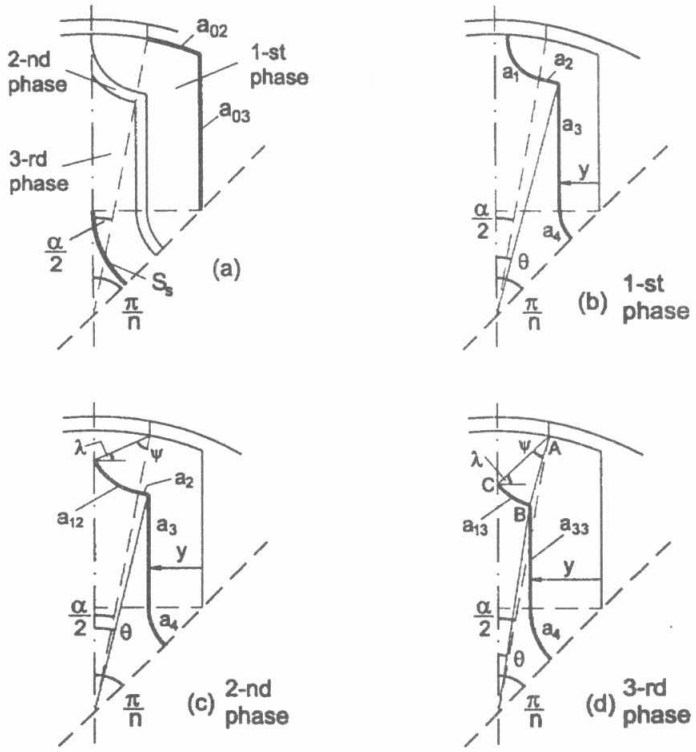

Fig. 4 Burning perimeter at different phases of burning

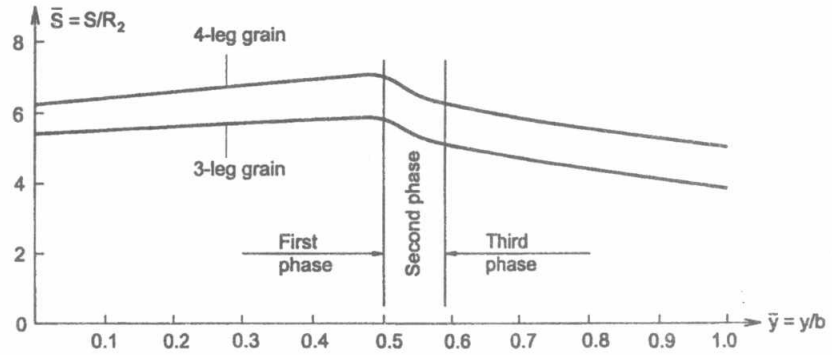

Fig. 5 The burning perimeter during the burning of flat surface grains

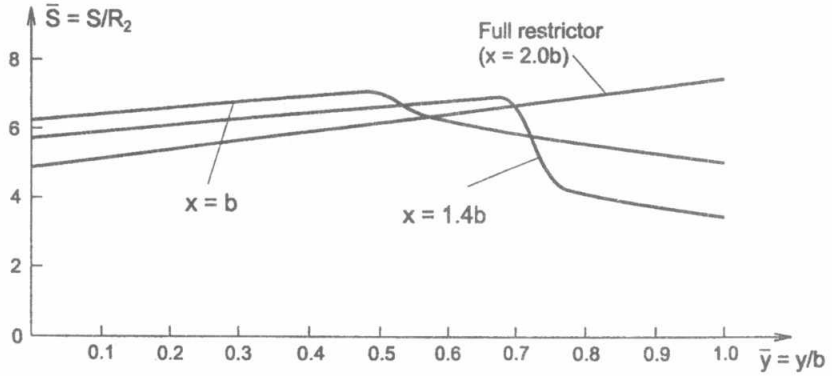

Fig. 6 The burning perimeters at different restrictor widthes for a 4-leg grain

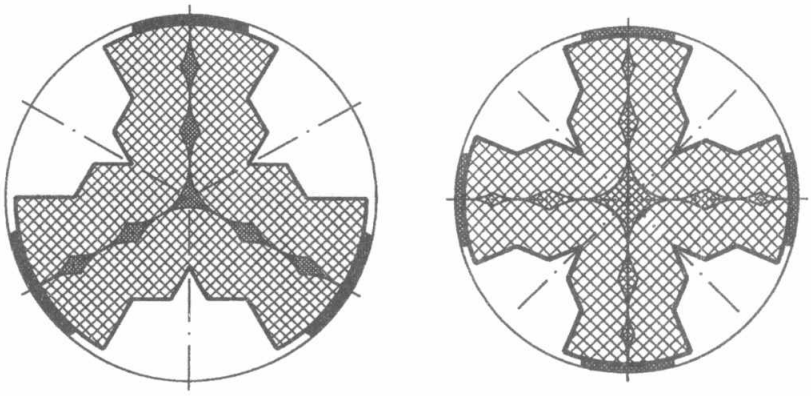

Fig. 7 Configuration of corrugated surface grains

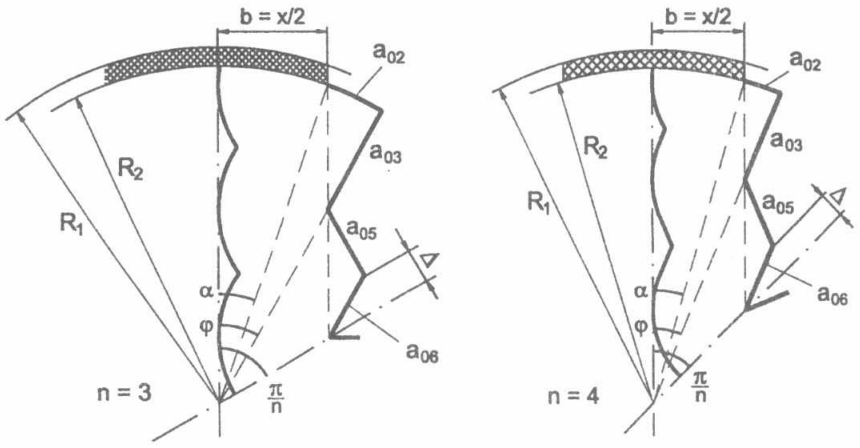

Fig. 8 Main dimensions of corrugated surface grains

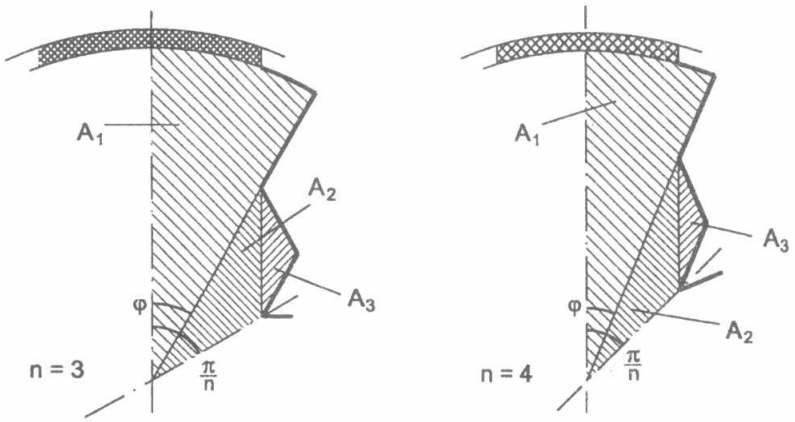

Fig. 9 Propellant cross-sectional area of corrugated surface grains

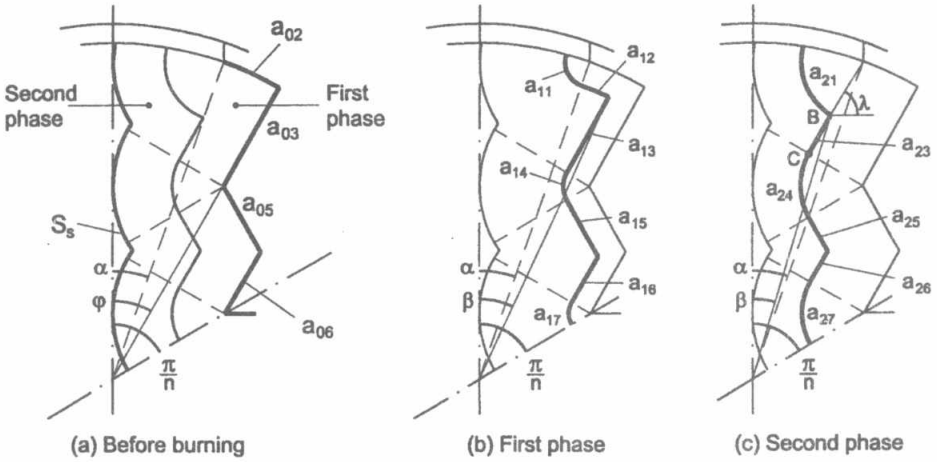

Fig. 10 Burning perimeters at different phases of burning

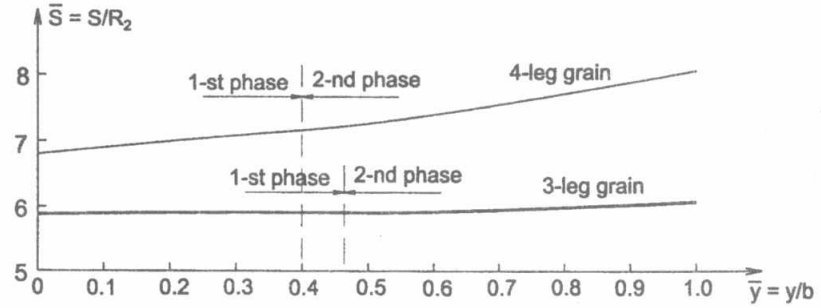

Fig. 11 The burning perimeters during combustion of corrugated surface grains

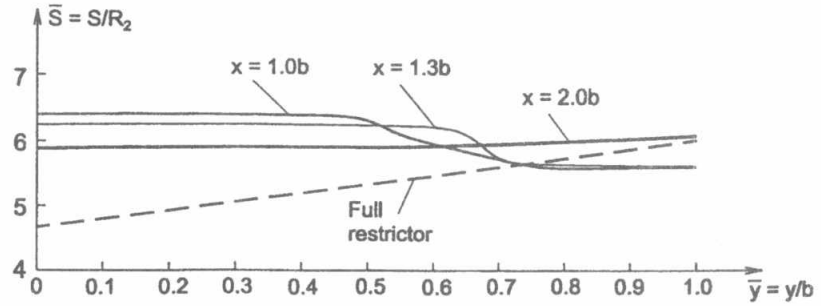

Fig. 12 The variation of the burning perimeter according to the restrictor width for a 3-leg grain